

DEVELOPING NOVEL METHODS TO IDENTIFY RNA-ASSOCIATED MECHANISMS FOR INHERITANCE

Zacharia Nabil Ettaki

Submitted to the faculty of the University Graduate School in partial fulfillment of
the requirements for the degree Master of Science in the department of
Biochemistry and Molecular Biology, Indiana University.

November 2020

Accepted by the Graduate Faculty, Indiana University or in partial fulfillment of
the requirements for the degree of Master of Science.

Master's Thesis Committee

Scott Aoki, D.V.M., Ph.D., Chair

Millie Georgiadis, Ph.D.

Lawrence Quilliam, Ph.D.

© 2020
Zacharia Nabil Ettaki

Zacharia Nabil Ettaki

DEVELOPING NOVEL METHODS TO IDENTIFY RNA-ASSOCIATED
MECHANISMS FOR INHERITANCE

Animals depend on inheriting non-genetic information early in life to grow and develop naturally. This inherited, non-genetic information was previously thought to be limited to DNA modifications and DNA binding proteins. But recent studies have expanded our understanding of inheritance to include RNA and RNA binding proteins. We currently lack methods to identify and enrich for RNA binding proteins that might be involved in providing non-genetic information from mother to daughter cells. Others have developed a method using modified enzyme tags to pulse-label proteins with small molecule fluorescent ligands and follow these proteins as they are inherited by cells. Here I characterized and tested the application of a fluorescent small molecule targeting antibody to enrich for these labeled proteins. I first tested the ability of this antibody to bind to fluorescent ligand-labeled enzymes. I determined that the antibody can efficiently bind to at least one of the labeled enzymes. Second, I determined crystallization conditions for the ligand binding antibody fragment. This thesis sets the stage for structure determination and to test whether this antibody can work in vivo to enrich for RNA binding proteins involved in the delivery of non-genetic information to cells.

Scott Aoki, D.V.M., Ph.D., Chair

Table of Contents

List of Figures	vi
List of Abbreviations	vii
Introduction	1
Methods	9
Halo recombinant protein purification	9
Immunoprecipitation	10
Immunoblot	10
Fab generation and purification	11
Crystallization	11
Results	12
Rhodamine antibody immunoprecipitation of TMR-labeled SNAP and Halo proteins	12
Crystallization of a rhodamine-binding Fab	13
Discussion	15
References	29
Curriculum Vitae	

List of Figures

Figure 1. Crystal structures of SNAP and Halo bound to their ligands	18
Figure 2. Chemistry of TMR fluorescence	19
Figure 3. Enrichment of RNP complexes using Halo or SNAP fusion proteins	20
Figure 4. Antibody Diagram	21
Figure 5. Halo protein purification	22
Figure 6. Schematic of the immunoprecipitation protocol	23
Figure 7. Immunoblot of Halo immunoprecipitation with a rhodamine-binding antibody	24
Figure 8. Immunoblot of Halo immunoprecipitation with a rhodamine-binding antibody.....	25
Figure 9. Rhodamine antibody cleavage and Fab purification	26
Figure 10. Crystals of a rhodamine-binding Fab	28

List of Abbreviations

DNA:	Deoxyribonucleic Acid
RNA:	Ribonulceic Acid
mRNA:	Messenger RNA
HATs:	Histone Acetyltransferases
NRDE-1:	Nuclear RNAi Defective – 1
H3K9:	Histone 3 Lysine 9
RNP:	Ribonucleoproteins
TDP-43:	TAR DNA Binding protein – 43
Agos:	Argonaute protein
RNAi:	Interference RNA
siRNA:	Short-interfering RNA
saeg-2:	Suppressor of Activated EGL-4 – 2
BG:	Benzylguanine
TMR:	Tetramethylrhodamine
Halo:	HaloTag
SNAP:	SNAPtag
H3:	Histone 3
CAF-1:	Chromatin Assembly Factor – 1
CENP-A:	Centromere Protein A
PCSK9:	Proprotein Convertase Subtilisin-like Kexin Type 9
GFP:	Green Fluorescent Protein
IgG:	Immunoglobulin G
Fc:	Fragment Crystallizable Region
Fab:	Antigen-binding Fragment
CDR:	Complementary Determining Region
H:	Heavy Chain
L:	Light Chain
mAb:	Monoclonal Antibody

Ab:	Antibody
LB:	Luria-Bertani
IPTG:	Isopropyl β - d-1-thiogalactopyranosid
BL21:	Bacterial Strain
g:	Gravity
HEPES:	Hdroxyethyl Piperazineethanesulfonic Acid
NTA:	Nitrilotriacetic Acid
SDS-PAGE:	Sodium Dodecyl Sulfate Polyacrylamide Gel Electrophoresis
SEC:	Size Exclusion Chromatography
FPLC:	Fast Protein Liquid Chromatography
kDa:	Kilo Dalton
PBS-T:	Phosphate Buffered Saline – Tween 20
PVDF:	Polyvinylidene Difluoride
PEG:	Polyethylene Glycol

Introduction

Progeny depend on the information passed on by their parents. This information provides a biological program for development into an adult organism and protection from disease. Without proper inheritance of this information, developmental defects and disease run rampant. While DNA and DNA modifications are a primary source of inherited information, recent studies have determined that RNA also plays a role (Posner et al., 2019; Vogler et al., 2018). My thesis aims to develop new tools to identify novel RNA-associated mechanisms for how animals inherit information.

Classically, we think of DNA, DNA modifications, and modifications to DNA binding proteins to be the information inherited from cell to cell and parent to child. These DNA and DNA binding protein modifications occur under the umbrella of “Epigenetics.” Epigenetics can regulate what is or is not expressed by changing these DNA and protein modifications without altering the underlying genetic code (Allis & Jenuwein, 2016). One example is the Histone Acetyltransferases (HATs). HATs add acetyl groups onto histones and can activate genes bound to these acetylated histones (Allis & Jenuwein, 2016). RNA regulatory mechanisms also can regulate DNA-associated epigenetics. For example, small RNAs and their binding proteins affect lysine histone modifications. NRDE-1, a small RNA binding protein, translocates to the nucleus and uses its RNA to target specific genes. A histone methyl transferase recruited by NRDE adds methyl groups to Histone 3 (H3K9) to promote formation of heterochromatin (Guérin et al., 2014). Thus, epigenetics includes mechanisms outside of direct DNA modifications.

Recently, several studies have modified the concept of epigenetics to include RNA-mediated regulation and RNA-protein complexes. *Vogler et al.* looked at the role of ribonucleoproteins (RNPs) and how they can direct cell differentiation (Vogler et al., 2018). The RNA binding protein TDP-43 was found to be highly active during muscle repair. During simulated muscle damage, they found TDP-43 to be in complex with mRNAs associated with muscle repair (Vogler et al., 2018). These TDP-43 and mRNA assemblies, dubbed “myo-granules,” were upregulated

during times of muscle growth and essential for cell survival. Myo-granules are proposed to have a significant role in cell differentiation and, when left uncleared, may contribute to muscle myopathies (Vogler et al., 2018).

In *C. elegans*, an RNA-protein complex plays a significant role in determining worm chemotactic behavior when searching for food during stressful times (Posner et al., 2019). RNAi is a broad term used to encompass many different types of Argonaute proteins (Agos) that bind small RNAs to reduce or silence expression of specific mRNAs (Lodish et al., 2008). In worms, small RNAs with their Agos are necessary for gametogenesis and embryonic formation (Grishok, 2005). The RNA portion of Ago serves as a guide to identify complementary mRNAs and repress their expression. Posner and colleagues recently showed that Ago RNAs are involved in inherited behavior (Posner et al., 2019). RDE-4, a double stranded RNA binding protein, works upstream to generate Ago-bound RNAs that act on the *saeg-2* gene to alter worm behavior. Change to *saeg-2* regulation occurs in response to external stimuli or internal nutritional states (Posner et al., 2019). These Ago small RNAs are created neuronally and can travel to the germline where they can repress genes, and subsequently the behavior of their progeny (Posner et al., 2019). In summary, new insights show that RNA-protein complexes play a key role in influencing cell development and organism behavior. These examples highlight that both RNA and RNA binding proteins facilitate cell or organism inheritance. I speculate that transmission of this inherited information must occur as RNA-protein complexes to preserve RNAs from degradation.

The biology and methods available in *C. elegans* make it an organism of choice for studying basic questions in RNA biology. The nematode is translucent to allow easy visualization of its cells, requires modest resources to live, and has a short generational time to study inheritance questions. Furthermore, new methods in molecular genetics enable genes to co-express robust protein tags (Juillerat et al., 2003; Los et al., 2008). Single gene editing is the process of inserting or altering a gene at its authentic locus. We can currently perform single

gene editing in *C. elegans* through Mos1 transposon-mediated modification or sequence-specific CRISPR/Cas9 (Nance & Frøkjær-Jensen, 2019). So, molecular methods are available to manipulate the *C. elegans* genome to express tags useful for imaging and tracking of protein components.

Two fusion protein tags that can be expressed in *C. elegans* are Snap and Halo. Both fusion proteins are optimal tools for protein labeling and cell imaging. Halo is derived from a bacterial haloalkane dehalogenase enzyme that reacts with haloalkane derivatives (Figure 1A) (Los et al., 2008), and SNAP is a modified alkylguanine-DNA transferase that reacts with benzyguanine (BG) derivatives (Figure 1C) (Juillerat et al., 2003). Mutations in both enzyme active sites trap substrates as covalent intermediates (Figure 1B and 1D) (Juillerat et al., 2003; Los et al., 2008), preventing ligand dissociation. Synthetic commercial ligands with substrates attached to fluorescent molecules (e.g. tetramethylrhodamine, TMR) can substitute for its normal substrates, allowing labeling of tagged proteins. These tags can be expressed with a protein of interest.

Others have used the SNAP and Halo tags to specifically label proteins and follow their stability in organisms over time. One group looked at how dynamic chromatin organization interacts with specific histone variants (H3.1 and H3.3) by using siRNA to knockdown expression of the histone chaperone CAF-1 and SNAP labelling the histone chaperone HIRA to visualize its specific function (Clément et al., 2016). Another group looked at how SNAP labelling could be a method to measure biological functions by measuring the half-life of various extra- and intracellular proteins (Bojkowska et al., 2011). Additionally, they demonstrated that *in vivo* SNAP-labelled tumors could be visualized using near-infrared probes. Finally, a pulse-chase assay was used with a SNAP-tagged H3 histone variant (Jansen et al., 2007), centromere protein A (CENP-A). CENP-A helps form centromere chromatin and subsequently its exit from mitosis. In both of these studies, ligands were pulsed in cells or animals, showing that enzyme-labelled proteins can be visualized and studied for their stability and movement within cells or animals. Halo protein has also been shown to be an effective tool to study protein stability and

cellular dynamics. One group looked at the role of proprotein convertase subtilisin-like kexin type 9 (PCSK9) in both intracellular and extracellular locations by pulsing with a cell impermeable and cell permeable fluorophores to visualize the functions on the inside and outside of the cell, respectively (Fischer, 2013). Li and colleagues were able to use Halo to study the dynamics of secretory granules through a Zinc fluorescent indicator (Li et al., 2015). Historically, green fluorescent protein (GFP) is the gold standard for protein imaging (Dunst & Tomancak, 2019)(Lavis & Raines, 2008). While GFP can be an optimal tag for protein visualization, it does not have multiple functionalities like SNAP or Halo. GFP also cannot be pulse labeled through chemical modification as described for SNAP or Halo in previous examples. In short, the SNAP and Halo tags provide a fantastic tool for fluorescent imaging and protein dynamics in cells and organisms like *C. elegans*.

Imaging and following proteins of interest *in vivo* with SNAP or Halo requires the use of a fluorescent small molecule. Small molecule fluorescence is defined as the emission of a photon upon excitation of a fluorophore (reviewed in (Dunst & Tomancak, 2019) and (Lavis & Raines, 2008)). The absorption of photons excites the fluorophore from its ground state (Figure 2A). The photon returning to its ground state causes a fluorescence signal (Figure 2A). The extinction coefficient is the probability that a fluorophore will absorb a photon. Fluorophores with high extinction coefficients are brighter than ones with low extinction coefficients and tend to be useful when light intensity needs to be kept to a minimum, such as when imaging living tissues or when there are very few fluorophore molecules (Lichtman & Conchello, 2005). Quantum yield is the ratio of fluorescence emission to nonradiative energy losses (Lichtman & Conchello, 2005). It is a direct measure of the efficiency of turning absorbed light into emitted light (Christian et al., 2013). For example, TMR, a derivative of xanthene dyes, has a quantum yield of 0.68 in aqueous solutions and has an emission of around 550 nm (Lavis & Raines, 2008). This lower quantum yield is likely due to the decay of the excited state around the rotation of the aromatic ring on TMR (Figure 2B). Preventing this ring from rotating can either promote or inhibit fluorescence, dependent on the ring position (Figure 2B). Studies with Fluorescein, a fluorescent molecule with a similar chemical

structure to TMR, have shown that maintaining the fluorophore in a certain position can quench fluorescence (Gayda et al., 2016). Increasing fluorophore rigidity in a specific position can come from the internal chemical structure (Lavis & Raines, 2008) or externally through fluorophore binding proteins, like antibodies.

Small molecule fluorescence can be used to visualize movement and effect of RNA-proteins complexes *in vivo*. Using a fluorescent fluorophore, such as TMR, we can tag and visualize RNA-protein complexes (Figure 3). This method allows for easy visualization of the movement of those RNA-protein complexes, but to study and characterize the RNA within the complex we need to enrich and isolate them. This can be done with antibodies (Figure 3). Using an antibody to specifically bind and pulldown complexes is called immunoprecipitation and has been used as a reliable and effective way to isolate and purify proteins of interest (Verhelst et al., 2015).

Antibodies are critical biological tools. They have a wide range of uses from isolating proteins out of solution, to modifying small molecule fluorescence. In biology, they are central to the adaptive immune system. In research, they are also important markers and reagents used for studying the identification and labeling of biological molecules. There are five classes of antibodies: IgA, IgM, IgG, IgD, and IgE. Each class plays a different role in the body in how and when they are expressed and how they work against disease. IgG is the predominant isotype found in the body and is made up of a light chain (~25 kDa) and heavy chain (~50 kDa) (Figure 4) (Adhikary et al., 2019). The general shape of IgG resembles the letter 'Y'. The bottom base of that 'Y' is called the Fc (Fragment constant) domain, while the two arms comprise the Fab (Fragment antigen binding) domain. IgG is comprised of four subclasses (IgG1-IgG4). IgG1 and IgG3 are both induced in response to protein antigens. IgG2 and IgG4 are associated with polysaccharide antigens (Schroeder & Cavacini, 2010). The four subclasses differ on the number of disulfide bonds they have. Disulfide bonds are formed between two cysteine residues in oxidizing conditions. They are what connects the light and heavy chains to each other (Figure 4). Disulfide bonds are broken by reducing agents. Partial

reduction of the disulfide bonds specifically at the hinge region connecting the CH2 domains causes an increased flexibility of the hinge and increased susceptibility to proteases (Schroeder & Cavacini, 2010). The Fc domain is primarily involved in binding to effector cells or activating other immune mediators such as complement (Schroeder & Cavacini, 2010). This Fc portion is how we define the isotype and subclass of the immunoglobulin (Schroeder & Cavacini, 2010).

The Fab domain specifically recognizes target molecules. The Fab contact surfaces are comprised of six complementary determining regions (CDR) or loops, three from the heavy chain and three from the light chain (Adhikary et al., 2019). Of these six loops, the heavy chain 3 (H3) loop is by far the most variable in length, sequence, and structure. CDR H3 can range between 1-35 amino acids in length. It can be almost 40% of the length of the Fab body itself (Adhikary et al., 2019). CDRs H3, H2, and L3 (light chain 3) make the largest contribution to interfacing with the antigen. L2 is notable for making the smallest and sometimes no contribution to the interface (Adhikary et al., 2019). A major research focus is understanding how antibodies recognize their target antigen. Structural biology has played a major role in this effort through determination of crystal structures of Fabs bound to their antigen targets. These structures show us to atomic resolution how antibody CDR loop amino acids interact with their antigens. In the case of fluorophore-binding antibodies, structures of fluorophore-antibody complexes will inform us how these antibodies change the conformation of the fluorophore to increase or decrease its fluorescence.

Much of our understanding how antibodies change fluorophore spectral properties come from work using Fluorescein-binding antibodies. Early studies showed how these antibodies can bind to their fluorophore targets (Bedzyk, Herron, et al., 1990; Bedzyk, Weidner, et al., 1990). Additionally, studying how antibodies bind to fluorescent ligands can give insight into how we can improve antibody binding interactions to small molecules. One such group studied fluorescein fluorescence quenching when bound to mAb 4-4-20 and found that increasing rigidity and decreased solvent accessibility improved quenching

(Swindlehurst & Voss, 1991). Another group determined crystal structures of Fabs bound to fluorescein (Bedzyk, Weidner, et al., 1990; Gayda et al., 2016). Their work showed that quenching is likely due to the antibody preventing planar rotation of the fluorophore's carboxyphenyl moiety (Figure 2B). Preventing rotation around this carboxyphenyl chemically has also been shown to quench fluorescence (Lavis & Raines, 2008). Of note, directed evolution of an antibody identified antibody mutations with an 1800-fold increase in binding affinity towards fluorescein (Midelfort, 2006). Crystal structures showed that mutations at the edge of the binding site lessened the negative charge repulsion between fluorescein and the antibody (Midelfort, 2006), presumably increasing binding affinity. Antibody-fluorescein binding was studied and it was found that in general, Tryptophan and Tyrosine residues are required for general binding in the active site of the antibody. Other residues (e.g. Serine, Histidine, Arginine, and Asparagine) are used for fine-tuning and binding specificity (Denzin et al., 1991). Recently, antibodies were identified to bind rhodamine (Eisold et al., 2015), a TMR relative. These antibodies are reported to enhance or quench fluorescence. I predict that the rhodamine-quenching antibody restricts planar rotation of rhodamine derivatives, similar to the fluorescein-quenching antibodies. There are no published structures of antibodies that enhance fluorophore binding, but I predict that a rhodamine-enhancing antibody promotes a planar conformation of the fluorophore. Additionally, structural characterization of these rhodamine antibodies should allow structure-based design of antibody mutations that enhance rhodamine affinity.

My research focuses on developing new molecular tools to identify information associated with RNA-protein complexes. Recently, others in the lab have been using Halo- and SNAP-tagged RNA binding proteins and TMR ligands to label and follow these proteins during cell development. The long-term vision is to be able to use molecular reagents like antibodies to enrich for these TMR-labeled RNA-protein complexes to determine their RNA targets (Figure 3). As discussed previously, others have identified antibodies that bind rhodamine (Eisold et al., 2015), a TMR relative. Thus, if we are able to use rhodamine-related ligands to label proteins, we can potentially use rhodamine-binding antibodies to enrich for

these complexes (Figure 3). My work determined the usefulness of a rhodamine-binding antibody for imaging and immunoprecipitation of TMR-labeled proteins. First, I used pull-down assays to determine whether this antibody can enrich for TMR-labeled Halo or SNAP tags. Second, I attempt to use x-ray crystallography to determine how this antibody binds to rhodamine. The structure will inform us how the antibody recognizes this small molecule and affects its fluorescence. Based on my results, we conclude that the antibody can be used to enrich for TMR-bound Halo but not SNAP. I identified preliminary conditions to crystallize a rhodamine binding Fab. Additional optimization will be needed for usable crystals for structure determination. Regardless, my work sets the stage to use this antibody as a new tool to study RNA-protein complexes *in vivo*.

Methods

Halo recombinant protein purification

His-tagged SNAP recombinant protein was a gift from Judith Kimble (Figure 5A). Halo protein was purified from recombinant sources. Briefly, a pET21a(+) vector expressing a his-tagged Halo (pDDC40) was transformed into BL21 E. coli (Thermo Scientific) and selected by Ampicillin. Transformed bacteria were cultured in LB broth (1% (bacto)-tryptone, 0.5% yeast extract, 1% NaCl) at 37°C, 225 rpm until the A600 Optical Density was between 0.4 - 0.8, as detected with an Ultrospec 3100 pro spectrophotometer (GE Amersham Biosciences). Bacteria were induced with 0.1 mM Isopropyl β - d-1-thiogalactopyranosid (IPTG), cultured at 16°C and 160 rpm, and collected after 16-18 hours incubation. Samples were collected, centrifuged at 5500xg for 10' and 3200xg for 30 minutes at 4°C, and frozen in liquid nitrogen. The bacterial pellet was stored at -80° C until use.

For purification, pellets were thawed on ice and resuspended in HN300 buffer (20 mM HEPES pH 7.0, 300 mM NaCl) supplemented with 10 mM imidazole. Cells were lysed using a microfluidizer (Divtech Equipment Co.) on ice. Samples were centrifuged at 3200xg for 30 minutes at 4°C, and the supernatant incubated with nickel-NTA agarose beads (HisPur Ni-NTA Resin, Thermo Scientific). The slurry was added to a gravity column and washed with HN300 buffer supplemented with increasing concentrations (10 mM, 20 mM, and 40 mM) of imidazole. Proteins were then eluted off beads with HN300 buffer supplemented with higher concentrations of imidazole (60 mM, 80 mM, 100 mM, and 250 mM). The 60-250 mM imidazole fractions were run on SDS-PAGE to confirm presence of Halo protein and to visualize the relative purity of each fraction. Fractions were then dialyzed with a 3K MWCO dialysis membrane (Spectra/Por) in HN buffer (20 mM HEPES pH 7.0, 100 mM NaCl) overnight at 4°C, concentrated (Vivaspin Turbo 4, Sartorius), and purified by size exclusion chromatography (SEC) with an Enrich SEC 650 column (Bio Rad, 24 mL capacity, separation range of 5 kDa – 650 kDa) using an NGC FPLC Chromatography System (Biorad) (Figure 5B). SEC fractions were deposited in 0.5 mL portions. Fractions were analyzed by SDS-PAGE and

Coomassie staining (Figure 5C). Halo eluted at the approximate position expected for a 36 kDa protein based on previously run protein standards (Bio Rad). Those fractions with the most recombinant protein and least background were concentrated and used for experiments. Halo and SNAP were quantified by A280 absorbance using the NanoDrop 1000 spectrophotometer (Thermo Scientific). The proteins used are shown by SDS-PAGE and Coomassie staining on Figure 5A.

Immunoprecipitation

Purified SNAP or Halo recombinant protein were incubated with TMR ligand (Halo-TMR (Promega), SNAP-TMR (NEB)) at 4°C for 1 hour in PBS-T (1x PBS with 0.01% tween-20)(Figure 6). G71-DC7F5 IgG antibody (In Vivo; Eisold et al., 2015) was incubated with Protein G Sepharose beads (GE Healthcare) for 1 hour in PBS-T at 4°C (Figure 6). The antibody-bead and protein-ligand mixtures were then mixed together in Pierce Micro-Spin columns (Thermo Scientific) and incubated overnight at 4°C (Figure 6). Using the spin column, samples were then washed 6 times with PBS-T prior to elution from the beads using 2X SDS-PAGE sample buffer (Bio Rad) supplemented with β -mercaptoethanol (Acros Organics). Samples were analyzed by immunoblot (see below).

Immunoblot

Samples were run on SDS-PAGE gels, and proteins were transferred to polyvinylidene difluoride (PVDF) membranes using Transblot Turbo transfer packs (Bio Rad) in a Transblot Turbo Transfer System (Bio Rad). PVDF membranes were then blocked with 5% evaporated milk in PBS-T followed by overnight incubation in 5% evaporated milk PBS-T with anti-histidine antibody (Novus) at 4°C. The following day, the immunoblot was washed with PBS-T and incubated for 45 minutes in 5% evaporated milk PBS-T with horseradish peroxidase secondary antibody (R&D Systems Bio-technique) at 20°C. Membranes were washed again with PBS-T and developed using Luminal/Enhancer SuperSignal West Femto and SuperSignal West Pico chemiluminescence (Thermo Scientific). The developed membrane was imaged on a ChemiDoc MP imaging system (Bio Rad).

Fab generation and purification

The method and reagents to generate Fabs were from the Pierce Fab Preparation Kit (Thermo Scientific). To test antibody cleavage conditions by papain, hybridoma-derived G71-DC7F5 IgG antibody (In Vivo, Eisold et al., 2015) was incubated with cysteine-supplemented Digestion Buffer (Thermo Scientific) and agarose-immobilized papain (Thermo Scientific) at 37°C. Samples were collected over time and stored in 2x SDS-PAGE sample buffer (250 mM Tris pH 6.8, 25 mM EDTA pH 8.0, 25% glycerol, 5% SDS) at -20°C prior to analysis by Coomassie-stained SDS-PAGE. Gels were imaged with a ChemiDoc MP imaging system (Bio Rad).

For larger scale Fab purification, antibody was incubated with the digestion conditions determined previously, and the sample was purified with a Protein A column (Thermo Scientific) and Size Exclusion Chromatography (Enrich SEC 650, Bio Rad). Chromatography fractions were analyzed by SDS-PAGE. Those fractions primarily with Fab were collected, concentrated (3K MWCO, Sartorius), and used for structural studies.

Crystallization

Purified Fab (5 mg/ml) was screened for crystallization conditions using in-house grid and commercial sparse matrix crystal screens. The in-house grid screens varied pH (5-9), and different concentrations of Polyethylene glycol (PEG), salt (Sodium Citrate, Lithium Sulfate, Magnesium Sulfate, Ammonium Sulfate, and Sodium Malonate) and 2-methyl-2,4-pentanediol (MPD). We tried two commercial sparse matrix screens: JCSG+ (Nextal) and Natrrix (Hampton Research). Screens were set up in 96 well, sitting drop trays using an Oryx4 (Douglas Instruments). Crystals were observed after two weeks in 0.2 M Lithium Sulfate, 0.1 M Tris pH 8.5, 40% (v/v) PEG 400. Crystals were rod-like and less than 20 microns in length. We are currently following up the hit with secondary screens.

Results

Rhodamine antibody immunoprecipitation of TMR-labeled SNAP and Halo proteins

The goal was to develop a method to isolate TMR-labeled SNAP and Halo proteins (Figure 4). Others have used SNAP and Halo protein tags as tools to pulse label proteins in cell culture and track their stability over time (Bojkowska et al., 2011; Los et al., 2008). A method to specifically isolate older, labeled RNA binding proteins versus newly made, unlabeled protein would allow us to identify differences in their target RNAs (Figure 4).

Antibody G71-DC7F5 IgG (G71 IgG) specifically binds to rhodamine (Eisold et al., 2015). We speculated it could also bind to tetramethylrhodamine (TMR), a chemical relative of rhodamine and commercially available as a ligand for both SNAP and Halo. To test whether G71 IgG could bind to TMR-labeled SNAP or Halo recombinant proteins, we performed immunoprecipitation assays. For the assays, we used SNAP and Halo recombinant protein purified from bacteria (Figure 7 and Figure 8). Both proteins were labeled with TMR ligand, then immunoprecipitated with G71 IgG bound to Protein G Sepharose beads. For controls, I excluded TMR ligand or G71 IgG in parallel samples to show that immunoprecipitation was dependent on the presence of both TMR and antibody (Figure 7 and Figure 8). Samples were bound to the beads and washed extensively before elution and analysis by SDS-PAGE immunoblot (Figure 6). The last wash sample was also analyzed to demonstrate that the elution sample only included protein bound to the beads. An anti-his tag antibody was used to detect recombinant SNAP and Halo proteins. The secondary antibody also detected G71 IgG, labeling the heavy and light antibody chains (Figure 7 and Figure 8).

TMR-labeled SNAP protein did not immunoprecipitate (Figure 7). Labeled SNAP protein was incubated with G71 IgG and Protein G Sepharose beads and tested for immunoprecipitation. SNAP was not detected in the elution, but the antibody bound well to the beads (Figure 7). I tried several rounds of this immunoprecipitation experiment, varying temperature, order of addition, and time.

In the discussion below, I discuss potential reasons why SNAP protein did not immunoprecipitate and how we could improve the assay. I currently conclude that the SNAP is not amenable for immunoprecipitation with G71 IgG.

TMR-labeled Halo protein did immunoprecipitate (Figure 8). The immunoprecipitation assay was performed similarly to SNAP immunoprecipitation but worked on the first trial. TMR-labeled Halo protein was incubated with G71 IgG and Protein G Sepharose beads and again tested for immunoprecipitation. This time, both Halo and antibody were detected in the elution (Figure 8). Three distinct bands were in the elute lane. Two of these bands corresponded with light and heavy chain antibody, while the third band corresponded to Halo protein (Figure 8). Halo immunoprecipitation was not observed in the absence of TMR ligand or G71 IgG, as expected. Controls for Halo were the same as SNAP, I excluded TMR or antibody to determine if the immunoprecipitation was dependent on both of those elements. Varying the Halo/ligand and the antibody/Protein G bead binding time had little effect on immunoprecipitation. I discuss below the attributes of Halo that may allow G71 IgG immunoprecipitation versus SNAP. Regardless, I conclude the G71 IgG can be used to enrich for TMR-labeled Halo proteins.

Crystallization of a rhodamine-binding Fab

I sought to determine the crystal structure of G71 Fab bound to its rhodamine ligand to understand how the antibody interacts with the fluorophore and why G71 quenches fluorophore fluorescence (Eisold et al., 2015). Previous structural work of an antibody that quenched fluorescein, another chemical fluorophore, identified that the antibody locked a phenyl ring in a position that blocked fluorescence (Denzin et al., 1991; Gayda et al., 2016). I speculate that G71 works similarly with rhodamine and its chemical relatives. The structure will also allow us to rationally redesign the antibody-TMR binding interface to improve binding.

G71 Fab was optimized and purified under standard procedures (see Methods). Papain cleaves IgG into antigen binding (Fab) and structural (Fc) fragments. I optimized IgG cleavage with papain (Figure 9A) and used these conditions to generate Fab fragments for structure determination. A Protein A or G column was used to remove contaminating post-cleavage antibody Fc fragment, and size exclusion chromatography used as a final purification step (Figure 9B-C). Purified G71 Fab was used in crystallization trials using in-house grid and commercial sparse-matrix screens. After two weeks, small 3-dimensional, rod-like crystals, less than 20 microns in length, were observed by light microscopy (Figure 10). We are currently following up this crystallization hit by varying the salt and precipitant concentrations. I discuss below additional ideas to obtain diffraction quality crystals for structure determination and why the crystals took an unusually long time to grow.

Discussion

The focus of this thesis was to develop new methods to identify labeled RNA-protein complexes with the long-term goal of enriching for these complexes and identifying their associated RNA information. I approached this problem from two different angles. One was to test whether a rhodamine antibody, G71 IgG, could bind and enrich protein tags labeled with a rhodamine derivative. The other was to determine the structure of the rhodamine antibody bound to its ligand. I made progress in both approaches, and we are now poised to test the usefulness of this antibody for RNA-protein complex enrichment in biological samples.

My work determined that G71 IgG could be used to immunoprecipitate TMR-labeled Halo. I did not observe enrichment of TMR-labeled SNAP. This discrepancy may be due to several reasons. First, Halo exhibited a much stronger input signal than SNAP, implying that more Halo protein was used in the binding reactions. Further work should consider trying several different concentrations of Halo and SNAP to quantitatively estimate immunoprecipitation efficiency. Second, Halo binds to its ligand (TMR) better than SNAP (Halo, $2700000 \text{ M}^{-1} \text{ s}^{-1}$ (Los et al., 2008); SNAP, $6000 \text{ M}^{-1} \text{ s}^{-1}$ (Juillerat et al., 2003)). Better binding increases the chances of antibody binding to TMR-labeled protein. Last, Halo or SNAP binding to its ligand may change the shape or accessibility of TMR to the antibody. This could prevent the antibody from recognizing the ligand and prohibit immunoprecipitation. Regardless, my results suggest that Halo should be used as the fusion protein of choice for G71 IgG immunoprecipitation-related experiments.

The next logical step for immunoprecipitation is to move from *in vitro* to *in vivo*. G71 IgG enriched for TMR-ligand bound recombinant Halo protein. I suggest testing enrichment of Halo tagged proteins in cell culture or animals. Prior work demonstrated that similar enzyme tags could be used to label proteins and track their stability over time ((Hoelzel & Zhang, 2020; Li et al., 2015; Los et al., 2008). G71 IgG allows us to now enrich for these stable, labeled proteins to see if their protein binding partners or bound nucleic acid targets change over time. In the case of RNA-protein complexes, we may be able to use this labeling strategy and

immunoprecipitation to further our understanding of how RNA-protein complexes shape organism development.

I attempted to determine the structure of the G71 Fab antigen binding fragment in complex with rhodamine. This effort led to identification of a condition that formed small rod crystals of G71 Fab. These crystals are approximately less than 20 microns in length and most likely too small for structure determination. Further work should focus on optimizing the conditions to enlarge crystal size. Some ways to grow larger crystals include condition optimization and microseeding. Condition optimization refers to changing different elements in the conditions in which initial crystals were grown in. By slightly altering the pH, salt concentration, or precipitant concentration, we may be able to produce larger, higher quality crystals. Another method to grow larger crystals is microseeding (Oswald et al., 2008). Crystal formation requires first nucleation and then crystal growth. Microseeding provides nucleation to the crystal growth condition. By placing an already nucleated “seed” into solution, crystals now only need to grow. Crystals grew after two weeks. Crystal growth can be impacted by time required to form a crystal lattice or protein purity impeding nucleation and growth. Future efforts should work to improve protein purity.

The structure of G71 Fab bound to rhodamine will provide two key pieces of information. It will show us how this Fab binds to a small molecule. By understanding the binding structure of the antibody to its ligand, we may be able to improve its binding affinity through rational mutagenesis. Mutagenesis has been utilized to improve antibody-fluorescent ligand binding. One group used fluorescein-binding antibody 4-4-20 and site directed mutagenesis to increase antibody binding to fluorescein by 1800-fold (Midelfort, 2006). The crystal structure will also inform us why G71 quenches rhodamine fluorescence (Eisold et al., 2015). Previous structural work with fluorescein antibodies determined that the fluorophore is locked in a conformation that prevents fluorescence (Bedzyk, Herron, et al., 1990; Denzin et al., 1991). I predict that G71 also locks rhodamine and rhodamine derivatives in a similar conformation. Mutagenesis can be used to

test any fluorescence quenching model. Future work should also focus on determining the crystal structure of a different rhodamine antibody that enhances fluorescence (Eisold et al., 2015). Structural work is not available of antibodies that enhance fluorescein fluorescence. These two rhodamine structures will thus give us novel insight into how antibodies are capable of affecting small molecule fluorescent properties. Since locking the fluorescein carboxyphenyl group perpendicular to the xanthene moiety prevents fluorescence (Gayda et al., 2016), I predict that locking the carboxyphenyl group planar to the xanthene moiety will promote fluorescence. Additionally, having two antibody tools at our disposal may help in our efforts to enrich for labeled RNA-protein complexes.

The long-term goal is to develop methods that may be used to study the information delivered by RNA-protein complexes. As I discussed in the introduction, the term epigenetics now includes RNA-protein complexes that are passed from cell to cell, and even in some cases mother to progeny. How do these complexes shape an organism? Why are these complexes utilized? How important are they to organism development and survival? Answering these questions requires development of novel methods, like those investigated in this thesis, to isolate these RNA-protein complexes and push our understanding of inheritance further.

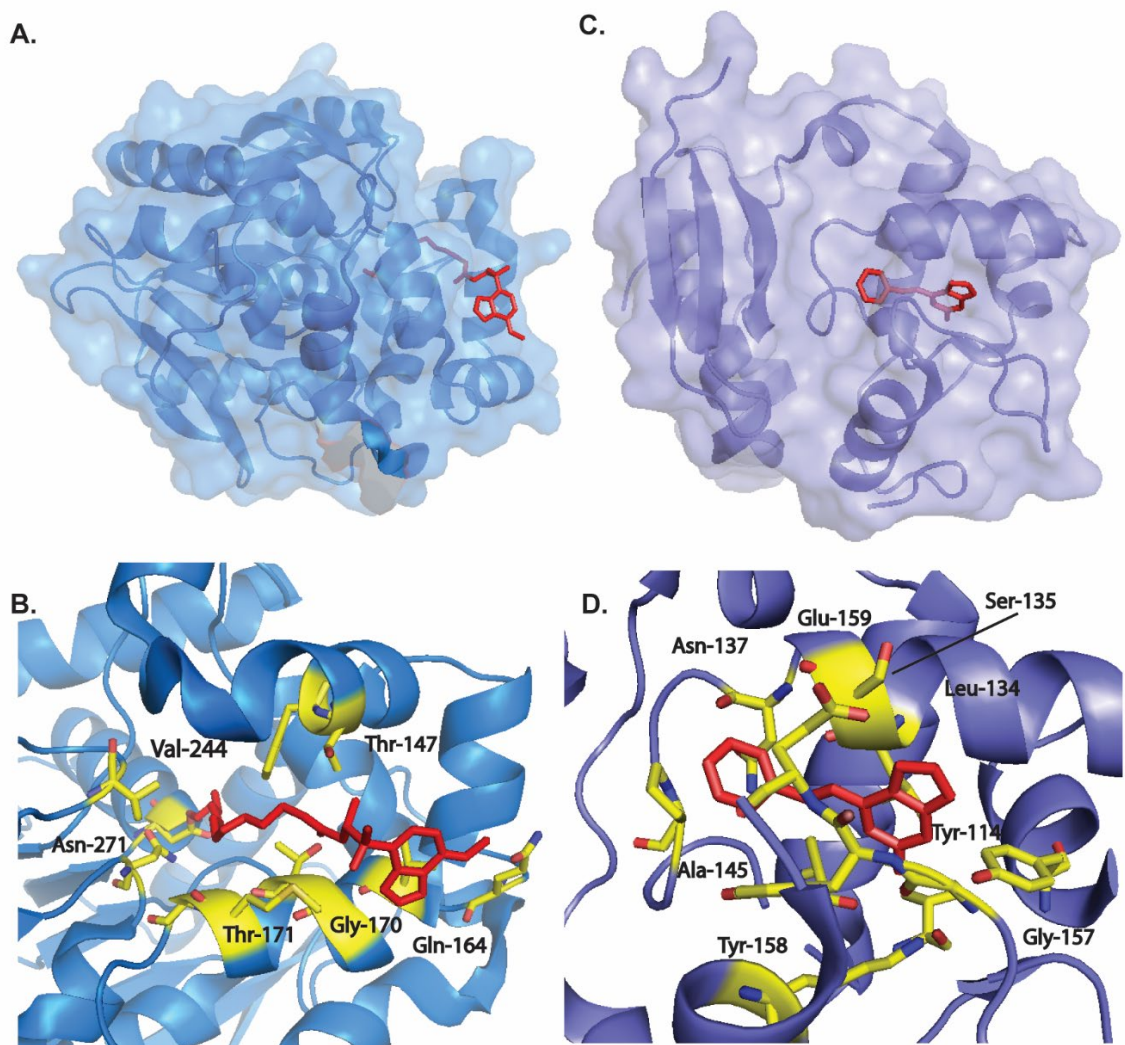


Figure 1. Crystal structures of SNAP and Halo bound to their ligands. (A) Crystal structure of Halo bound to its benzoxadiazole ligand (red). Modified from Kang and colleagues (PDB ID: 5Y2Y, Kang et al., 2017). (B) Molecular details of the Halo binding pocket interacting with the benzoxadiazole ligand (red). Interacting amino acid side chains forming hydrogen bonds and salt bridges are highlighted in yellow. (C) Crystal structure of SNAP bound to its benzyl guanine ligand (red). Modified from Schmitt and colleagues (PDB ID: 3KZZ). (D) SNAP-ligand amino acid side chain interactions (yellow) forming hydrogen bonds and salt bridges to the SNAP ligand (red).

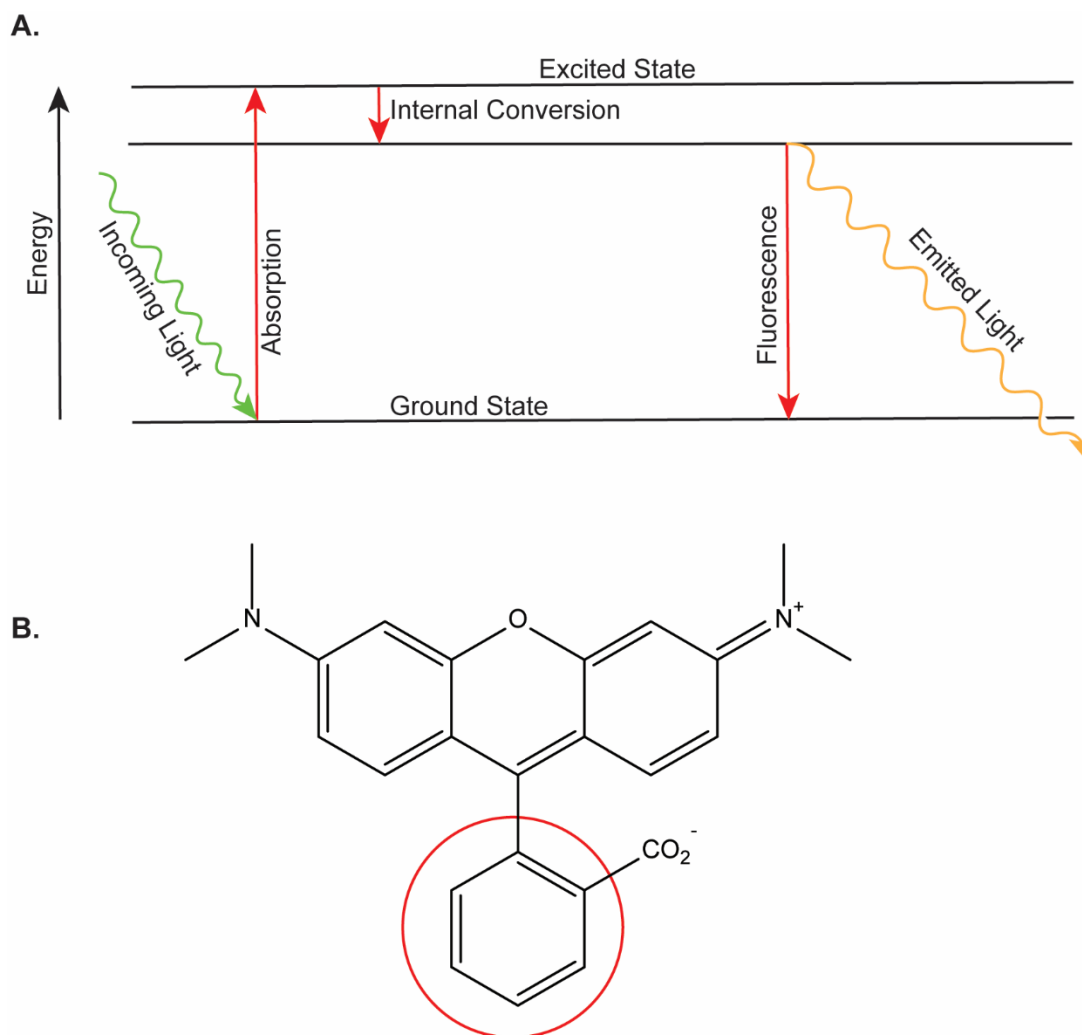


Figure 2. Chemistry of TMR fluorescence. (A) Fluorescence emission and excitation diagram. Through the absorbance of a specific wavelength of light (green arrow), the fluorophore increases its energy from its ground state to an excited state. At this point, internal conversion may occur. This is the act in which a higher vibrational energy is achieved while the molecule itself shifts to a lower electronic state. Fluorescence is achieved when shifting from the excited state back down to the ground state. As this happens, photons are emitted. Because of the release of some energy during internal conversion (small red arrow), the emitted light is released at a longer wavelength (less energy, yellow arrow). (B) Chemical structure of tetramethylrhodamine (TMR). Rotation of the benzyl ring located off the center ring of the xanthene moiety (circled in red) affects fluorescent emission.

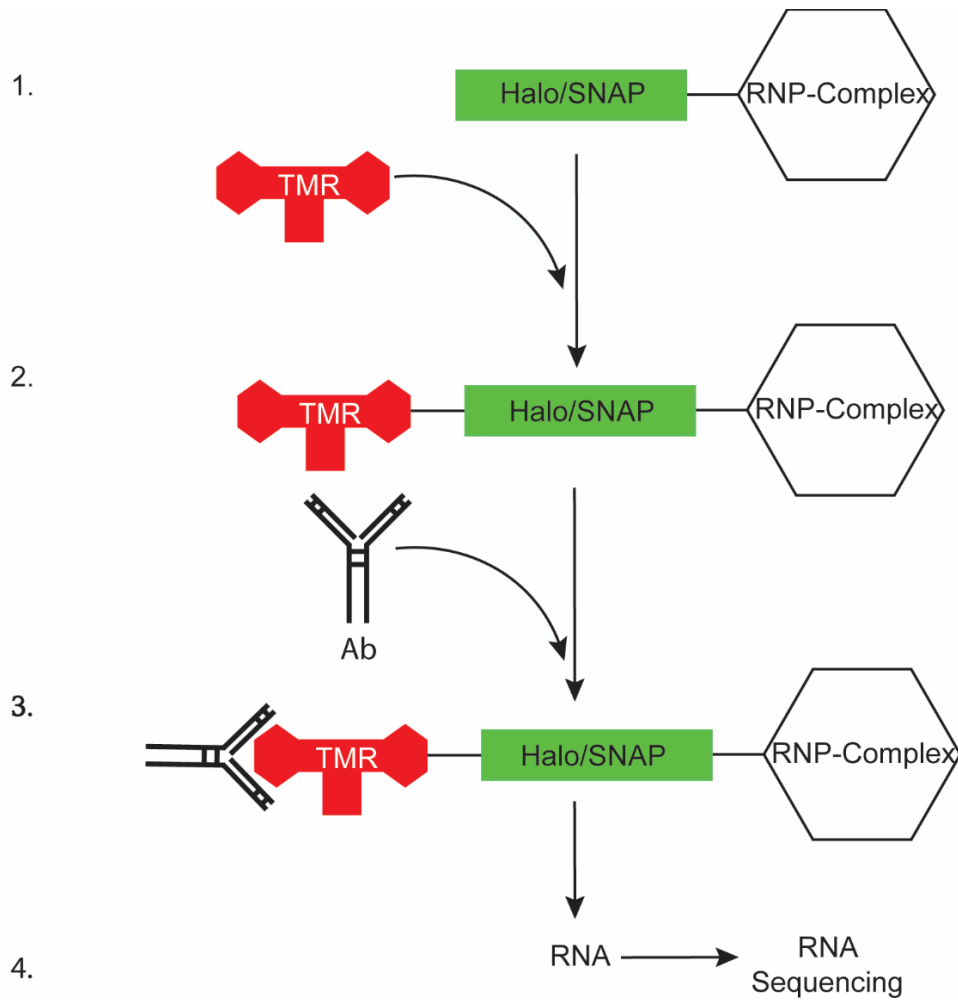


Figure 3. Enrichment of RNP complexes using Halo or SNAP fusion proteins. SNAP or Halo can be expressed with an RNA binding protein of interest. This permits labelling of the tags with a rhodamine derivative ligand (1). Using a rhodamine-binding antibody, TMR-bound RNA-protein complexes can be enriched from unlabeled complexes (2-3). Enriched samples can then be sequenced to identify bound RNA (4).

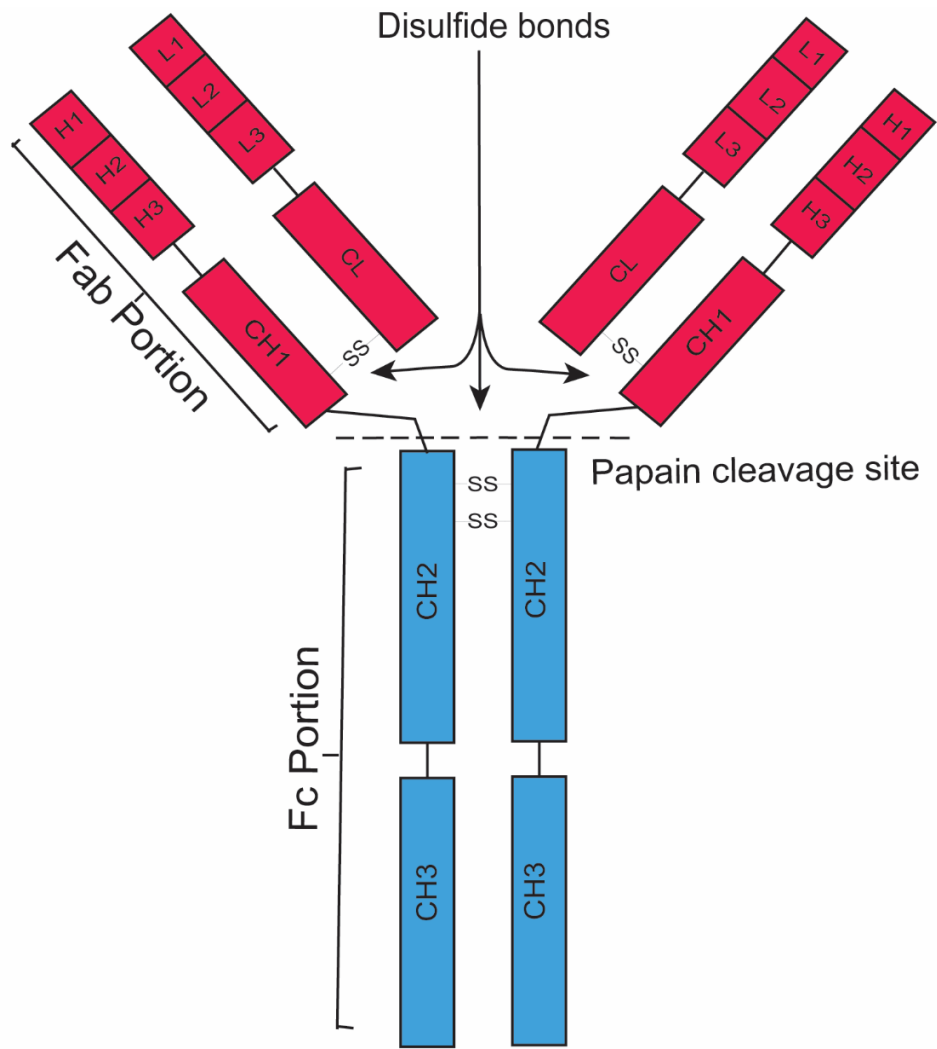


Figure 4. Antibody diagram. Fab and Fc portions labeled. Papain cleaves along the dotted line.

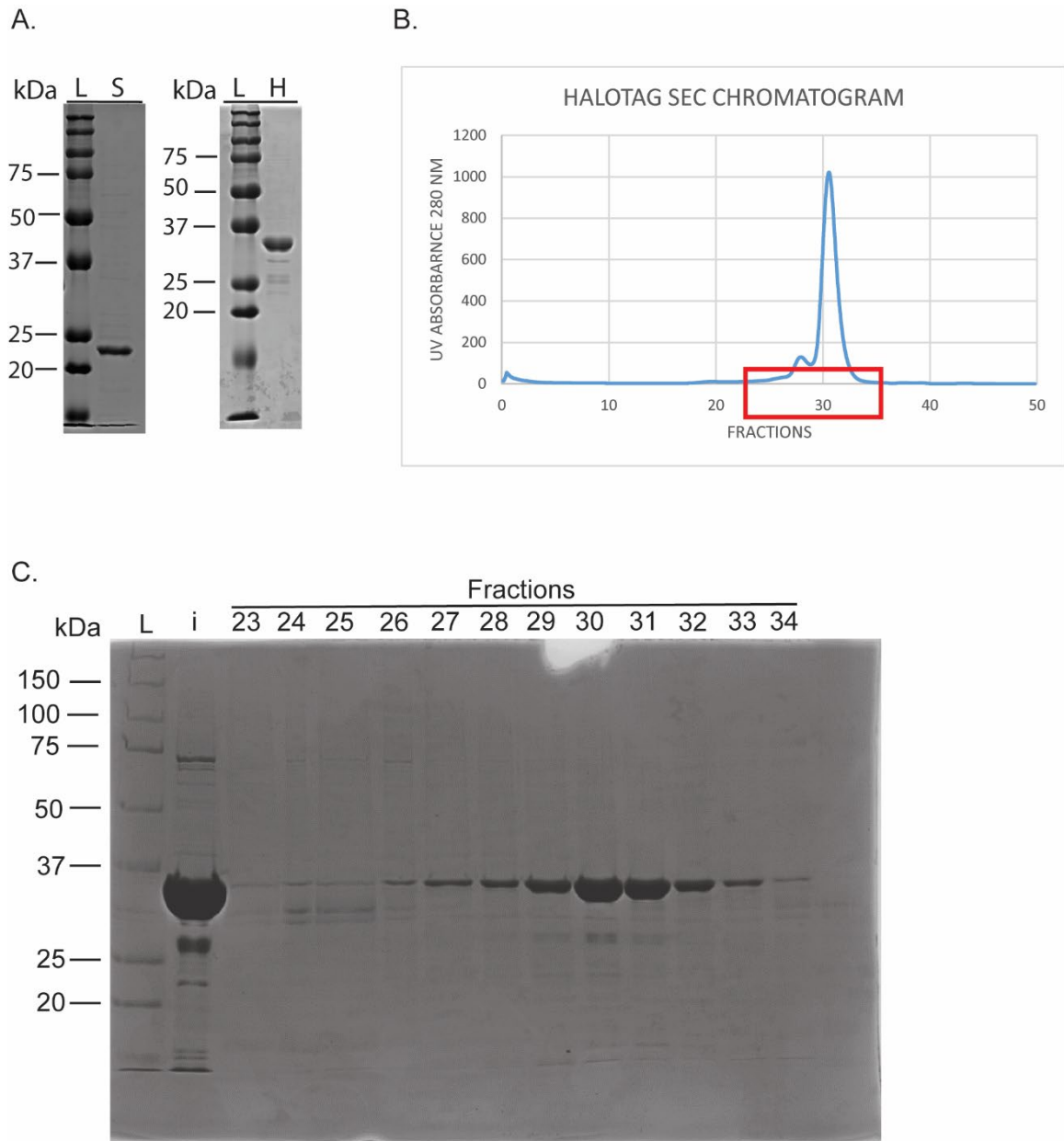


Figure 5. Halo protein purification. (A) SDS-PAGE gel showing expression of both SNAP “S” and Halo “H” fusion proteins next to protein ladder “L” measured in kilodaltons “kDa”. (B) Halo Chromatogram following SEC purification on FPLC. Fractions 23-34 were considered to have the most Halo protein and were run on SDS-PAGE to assess relative purity. (C) SDS-PAGE gel run with fractions from SEC purification. Of these fractions, 27-33 were concentrated and used in immunoprecipitation assay.

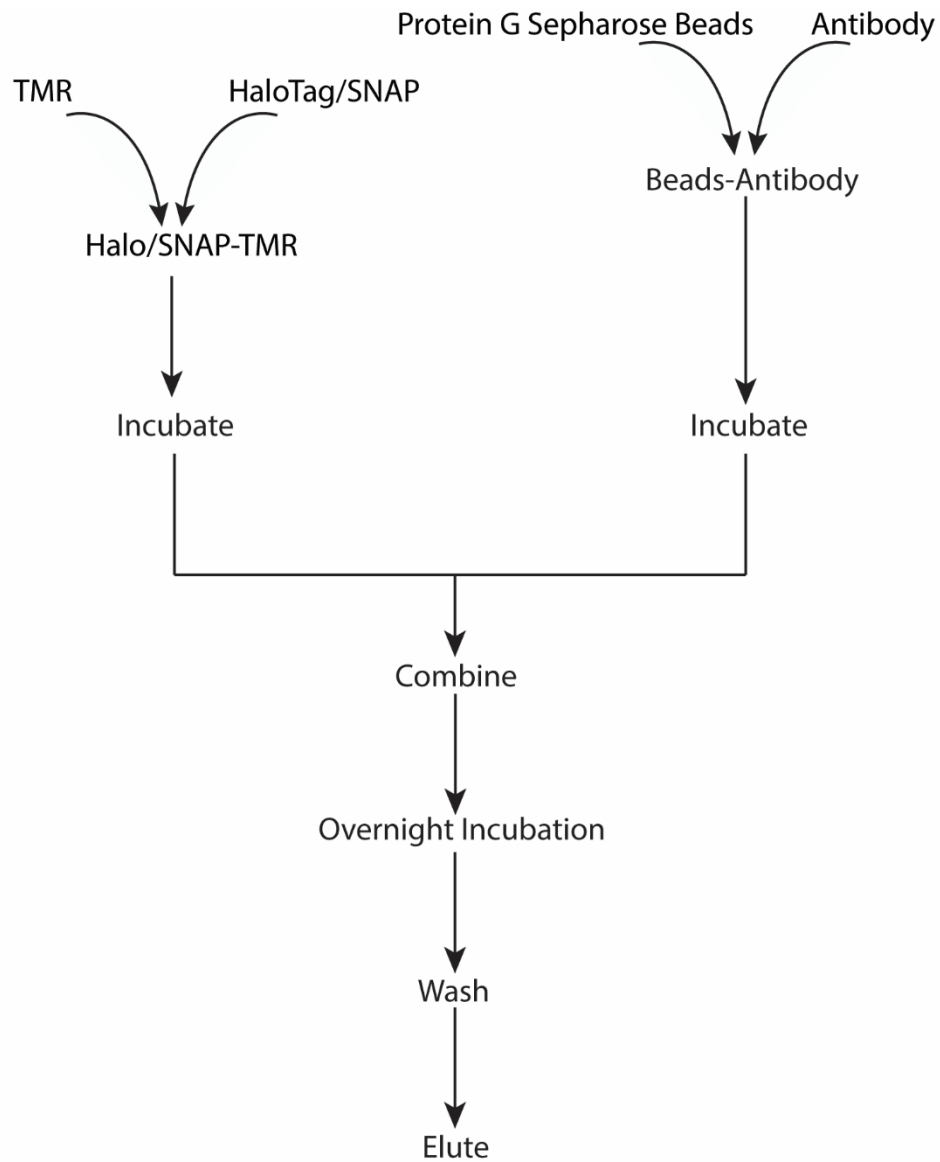


Figure 6. Schematic of the immunoprecipitation protocol. Fusion protein/TMR and beads/antibody pairs were incubated for an hour at 4°C. Both mixtures were combined and incubated overnight before being washed and eluted. Protein was visualized by immunoblot.

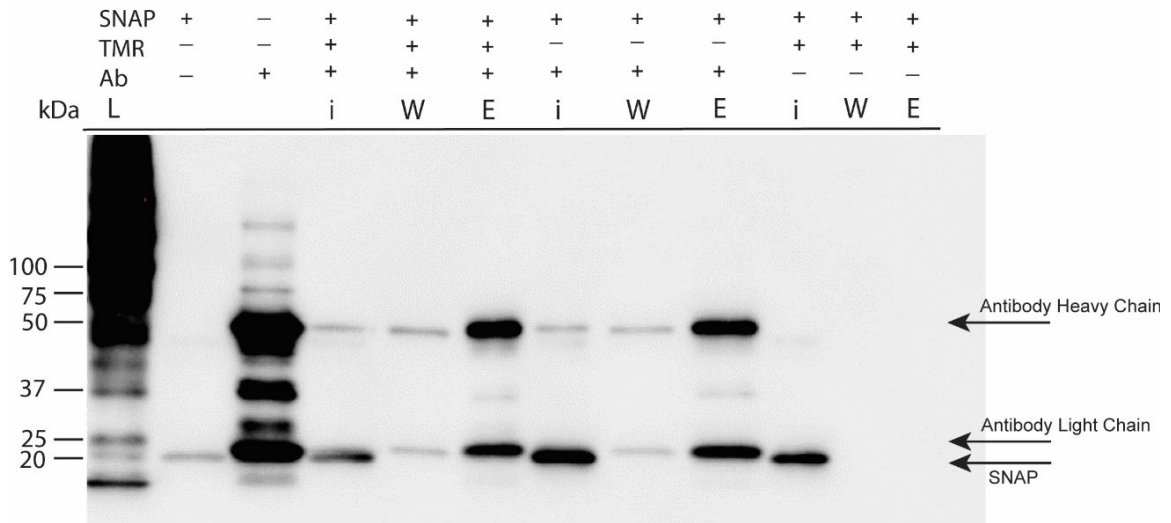


Figure 7. Immunoblot of a failed SNAP immunoprecipitation with a rhodamine-binding antibody. No SNAP band is visible in the elute. While SNAP protein was not found in the elute, antibody binds well to the beads. Antibody heavy and light chain are labeled alongside SNAP protein, which runs at just under light chain antibody. L, ladder; kDa, kilodaltons; i, initial unwashed sample; W, washed sample; E, eluted sample. Anti-histidine tag primary antibody.

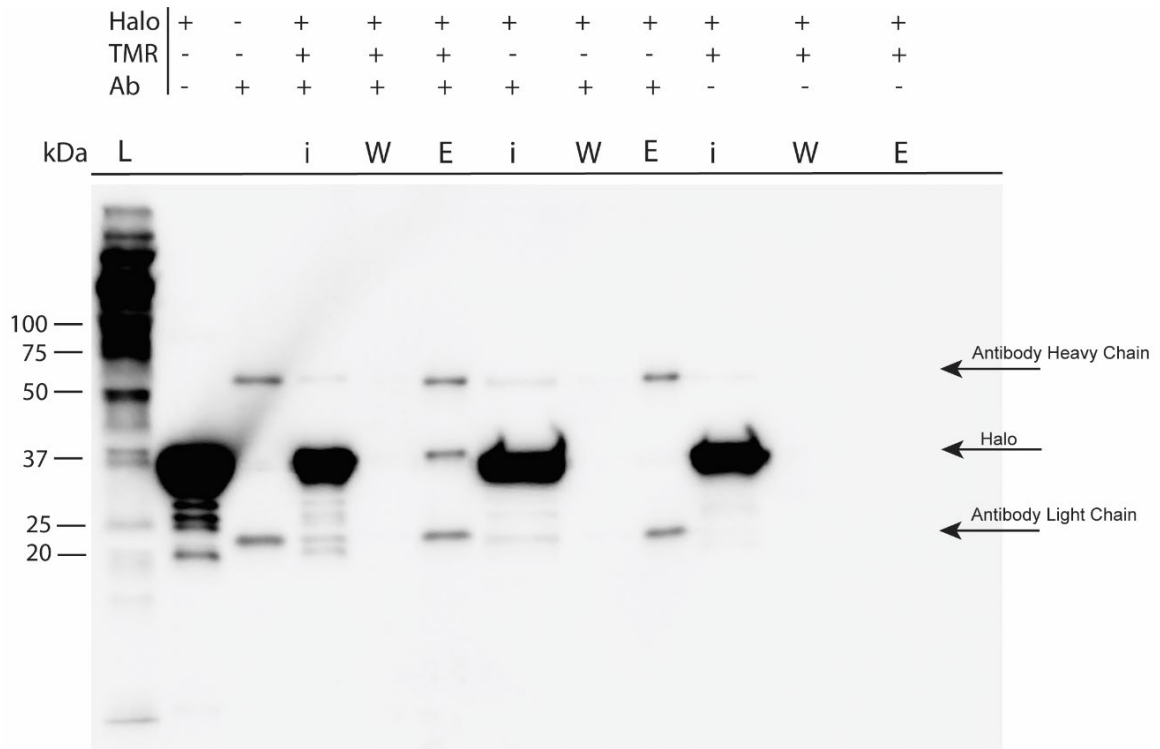


Figure 8. Immunoblot of Halo immunoprecipitation with a rhodamine-binding antibody. Each IP was washed before eluting with 2x SDS-Sample buffer. Controls determined if IP was dependent on either antibody or TMR by leaving one or the other out of the experiment. IP was depended on both antibody and TMR. Heavy and light chain antibody are labeled along with Halo protein, which runs between antibody bands. L, ladder; kDa, kilodaltons; i, initial unwashed sample; W, washed sample; E, eluted sample. Anti-histidine tag primary antibody.

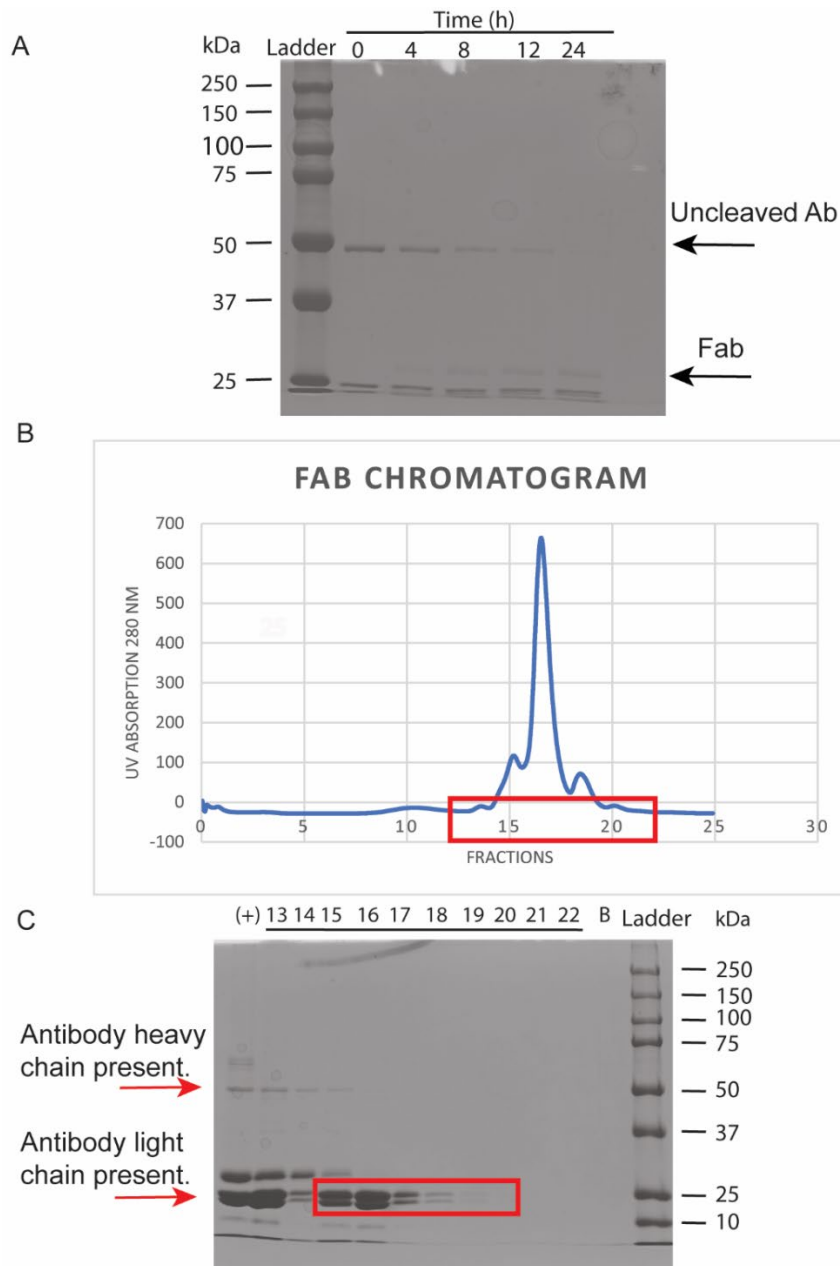


Figure 9. Rhodamine antibody cleavage and Fab purification. (A) Coomassie-stained SDS-PAGE gel of antibody cleavage time course with papain. Antibody was incubated with immobilized Papain resin and samples were collected over time. 50 kilodalton (kDa) bands represent uncleaved heavy chain and 25 kDa bands are light chain and cleaved Fab heavy chain fragments. h, hours. (B) Size exclusion chromatography (SEC) of papain-cleaved antibody. Protein was detected by UV absorption (A280). Fractions in the red box were analyzed by SDS-PAGE and Coomassie-staining. (C) Coomassie-stained SDS-PAGE gel of size

exclusion fractions. Numbered fractions correspond to chromatogram in (B). (+), sample after cleavage. B, blank gel lane. kDa, kilodaltons. Fractions 15-20 (red box) were concentrated and used for structural studies.

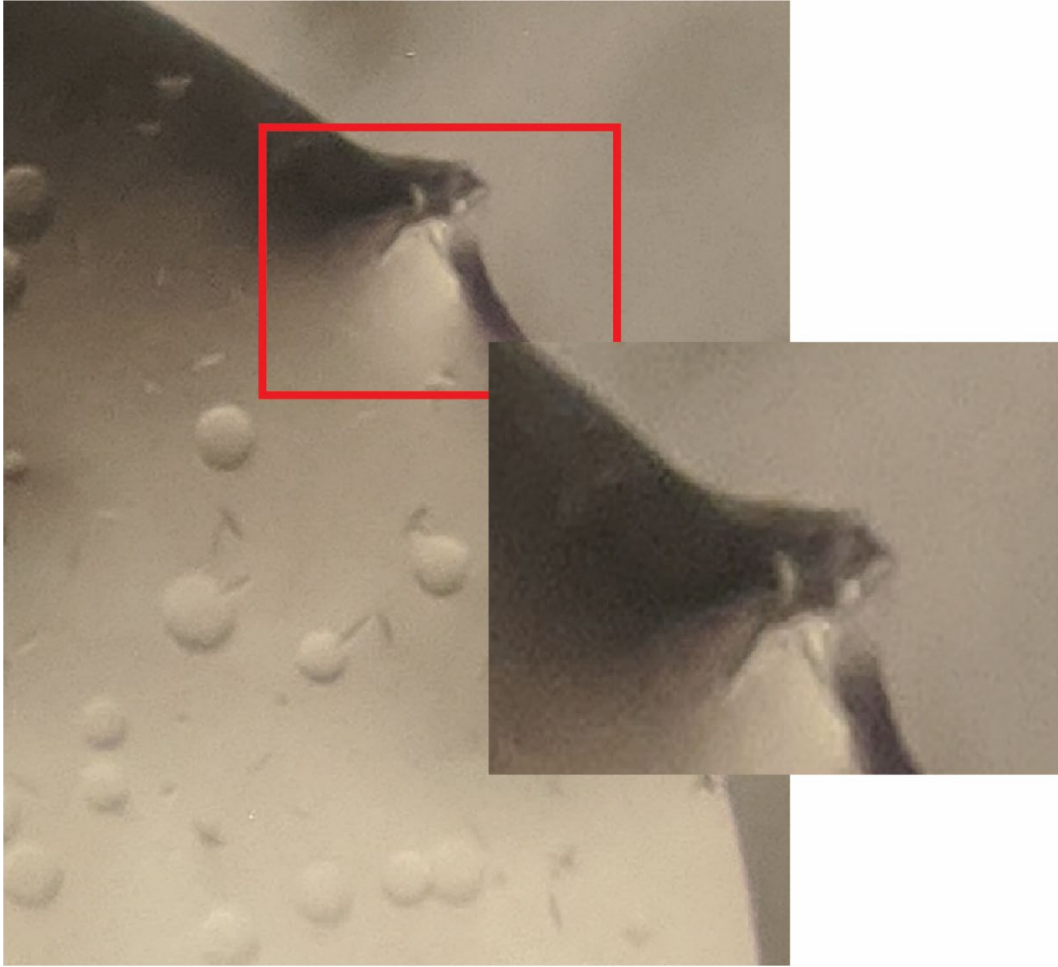


Figure 10. Crystals of a rhodamine-binding Fab. Crystals are rod-like and less than 20 microns in length. Circled in red is a large formation of several crystals. Round clear circles are phase separation.

References

- Adhikary, R., Zimmermann, J., Stanfield, R. L., Wilson, I. A., Yu, W., Oda, M., & Romesberg, F. E. (2019). Structure and Dynamics of Stacking Interactions in an Antibody Binding Site. *Biochemistry*, *58*(27), 2987–2995. <https://doi.org/10.1021/acs.biochem.9b00119>
- Allis, C. D., & Jenuwein, T. (2016). The molecular hallmarks of epigenetic control. *Nature Reviews Genetics*, *17*(8), 487–500. <https://doi.org/10.1038/nrg.2016.59>
- Bedzyk, W., Herron, J., Edmundson, A., & Voss, E. (1990). *Active Site Structure and Antigen Binding Properties of Idiotypically Cross-reactive Anti-fluorescein Monoclonal Antibodies*. The Journal of Biological Chemistry.
- Bedzyk, W., Weidner, K., Denzin, L., Johnson, L., Hardman, K., Pantoliano, M., Asel, E., & Voss, E. (1990). *Immunological and Structural Characterization of a High Affinity Anti-fluorescein Single-chain Antibody**. Journal of Biological Chemistry.
- Bojkowska, K., Santoni de Sio, F., Barde, I., Offner, S., Verp, S., Heinis, C., Johnsson, K., & Trono, D. (2011). Measuring In Vivo Protein Half-Life. *Chemistry & Biology*, *18*(6), 805–815. <https://doi.org/10.1016/j.chembiol.2011.03.014>
- Christian, W., Markus, G., Jutta, P., Monika, S., & Ute, R.-G. (2013). Relative and absolute determination of fluorescence quantum yields of transparent samples. *Nature Protocols*, *8*, 1535–1550. <https://doi.org/10.1038/nprot.2013.087>
- Clément, C., Vassias, I., Ray-Gallet, D., & Almouzni, G. (2016). Functional Characterization of Histone Chaperones Using SNAP-Tag-Based Imaging to Assess De Novo Histone Deposition. In *Methods in Enzymology* (Vol. 573, pp. 97–117). Elsevier. <https://doi.org/10.1016/bs.mie.2016.04.004>
- Denzin, L., Whitlow, M., & Voss, E. W. (1991). Single-chain Site-specific Mutations of Fluorescein-Amino Acid Contact Residues in High Affinity Monoclonal Antibody 4-4-20*. *The Journal of Biological Chemistry*, *266*(21), 14095–14103.
- Dunst, S., & Tomancak, P. (2019). Imaging Flies by Fluorescence Microscopy: Principles, Technologies, and Applications. *Genetics*, *211*(1), 15–34. <https://doi.org/10.1534/genetics.118.300227>
- Eisold, U., Sellrie, F., Schenk, J. A., Lenz, C., Stöcklein, W. F. M., & Kumke, M. U. (2015). Bright or dark immune complexes of anti-TAMRA antibodies for adapted fluorescence-based bioanalysis. *Analytical and Bioanalytical Chemistry*, *407*(12), 3313–3323. <https://doi.org/10.1007/s00216-015-8538-0>
- Fischer, P. (2013). Utilizing HaloTag Technology to Track the Fate of PCSK9 from Intracellular vs. Extracellular Sources. *Current Chemical Genomics*, *6*(1), 38–47. <https://doi.org/10.2174/1875397301206010038>
- Gayda, S., Longenecker, K. L., Judge, R. A., Swift, K. M., Manoj, S., Linthicum, D. S., & Tetin, S. Y. (2016). Three-dimensional structure, binding, and spectroscopic characteristics of the monoclonal antibody 43.1 directed to

- the carboxyphenyl moiety of fluorescein. *Biopolymers*, 105(4), 234–243. <https://doi.org/10.1002/bip.22801>
- Grishok, A. (2005). RNAi mechanisms in *Caenorhabditis elegans*. *FEBS Letters*, 579(26), 5932–5939. <https://doi.org/10.1016/j.febslet.2005.08.001>
- Guérin, T. M., Palladino, F., & Robert, V. J. (2014). Transgenerational functions of small RNA pathways in controlling gene expression in *C. elegans*. *Epigenetics*, 9(1), 37–44. <https://doi.org/10.4161/epi.26795>
- Hoelzel, C. A., & Zhang, X. (2020). Visualizing and Manipulating Biological Processes Using HaloTag and SNAP-Tag Technologies. *ChemBioChem*, cbic.202000037. <https://doi.org/10.1002/cbic.202000037>
- Jansen, L. E. T., Black, B. E., Foltz, D. R., & Cleveland, D. W. (2007). Propagation of centromeric chromatin requires exit from mitosis. *Journal of Cell Biology*, 176(6), 795–805. <https://doi.org/10.1083/jcb.200701066>
- Juillerat, A., Gronemeyer, T., Keppler, A., Gendreizig, S., Pick, H., Vogel, H., & Johnsson, K. (2003). Directed Evolution of O6-Alkylguanine-DNA Alkyltransferase for Efficient Labeling of Fusion Proteins with Small Molecules In Vivo. *Chemistry & Biology*, 10(4), 313–317. [https://doi.org/10.1016/S1074-5521\(03\)00068-1](https://doi.org/10.1016/S1074-5521(03)00068-1)
- Lavis, L. D., & Raines, R. T. (2008). Bright Ideas for Chemical Biology. *ACS Chemical Biology*, 3(3), 142–155. <https://doi.org/10.1021/cb700248m>
- Li, D., Liu, L., & Li, W.-H. (2015). Genetic Targeting of a Small Fluorescent Zinc Indicator to Cell Surface for Monitoring Zinc Secretion. *ACS Chemical Biology*, 10(4), 1054–1063. <https://doi.org/10.1021/cb5007536>
- Lichtman, J. W., & Conchello, J.-A. (2005). Fluorescence microscopy. *Nature Methods*, 2(12), 910–919. <https://doi.org/10.1038/nmeth817>
- Lodish, H. F. (Ed.). (2008). *Molecular cell biology* (6th ed). W.H. Freeman.
- Los, G. V., Encell, L. P., McDougall, M. G., Hartzell, D. D., Karassina, N., Zimprich, C., Wood, M. G., Learish, R., Ohana, R. F., Urh, M., Simpson, D., Mendez, J., Zimmerman, K., Otto, P., Vidugiris, G., Zhu, J., Darzins, A., Klaubert, D. H., Bulleit, R. F., & Wood, K. V. (2008). HaloTag: A Novel Protein Labeling Technology for Cell Imaging and Protein Analysis. *ACS Chemical Biology*, 3(6), 373–382. <https://doi.org/10.1021/cb800025k>
- Midelfort, K. S. (2006). Context-dependent mutations predominate in an engineered high-affinity single chain antibody fragment. *Protein Science*, 15(2), 324–334. <https://doi.org/10.1110/ps.051842406>
- Nance, J., & Frøkjær-Jensen, C. (2019). The *Caenorhabditis elegans* Transgenic Toolbox. *Genetics*, 212(4), 959–990. <https://doi.org/10.1534/genetics.119.301506>
- Oswald, C., Smits, S., Bremer, E., & Schmitt, L. (2008). Microseeding – A Powerful Tool for Crystallizing Proteins Complexed with Hydrolyzable Substrates. *International Journal of Molecular Sciences*, 9(7), 1131–1141. <https://doi.org/10.3390/ijms9071131>
- Posner, R., Toker, I. A., Antonova, O., Star, E., Anava, S., Azmon, E., Hendricks, M., Bracha, S., Gingold, H., & Rechavi, O. (2019a). Neuronal Small RNAs Control Behavior Transgenerationally. *Cell*, 177(7), 1814–1826.e15. <https://doi.org/10.1016/j.cell.2019.04.029>

- Posner, R., Toker, I. A., Antonova, O., Star, E., Anava, S., Azmon, E., Hendricks, M., Bracha, S., Gingold, H., & Rechavi, O. (2019b). Neuronal Small RNAs Control Behavior Transgenerationally. *Cell*, *177*(7), 1814-1826.e15. <https://doi.org/10.1016/j.cell.2019.04.029>
- Schroeder, H. W., & Cavacini, L. (2010). Structure and function of immunoglobulins. *Journal of Allergy and Clinical Immunology*, *125*(2), S41–S52. <https://doi.org/10.1016/j.jaci.2009.09.046>
- Swindlehurst, C. A., & Voss, E. W. (1991). Fluorescence measurements of immune complexes of Mab 4–4-20 with isomeric haptens. *Biophysical Journal*, *59*(3), 619–628. [https://doi.org/10.1016/S0006-3495\(91\)82277-9](https://doi.org/10.1016/S0006-3495(91)82277-9)
- Verhelst, J., De Vlieger, D., & Saelens, X. (2015). Co-immunoprecipitation of the Mouse Mx1 Protein with the Influenza A Virus Nucleoprotein. *Journal of Visualized Experiments*, *98*, 52871. <https://doi.org/10.3791/52871>
- Vogler, T. O., Wheeler, J. R., Nguyen, E. D., Hughes, M. P., Britson, K. A., Lester, E., Rao, B., Betta, N. D., Whitney, O. N., Ewachiw, T. E., Gomes, E., Shorter, J., Lloyd, T. E., Eisenberg, D. S., Taylor, J. P., Johnson, A. M., Olwin, B. B., & Parker, R. (2018). TDP-43 and RNA form amyloid-like myo-granules in regenerating muscle. *Nature*, *563*(7732), 508–513. <https://doi.org/10.1038/s41586-018-0665-2>

Curriculum Vitae

Zacharia Nabil Ettaki

Education

- Nov 2020 M.S. in Biochemistry and Molecular Biology; Indiana University-Purdue University Indianapolis, Indianapolis, IN
- May 2018 B.S. in Biology with minor in Chemistry; Washington State University, Pullman, WA

Positions and Employment

- 2019-2020 Graduate Student, PI: Scott Aoki, Indiana University School of Medicine
- Identify and study novel methods relating to protein-RNA inheritance.
 - Protein culture and purification via size exclusion chromatography.
 - X-ray crystallography to resolve protein structure.
 - Western blot, SDS-PAGE, gel electrophoresis as related to proteins.
 - Development of an immunoprecipitation assay.
- 2016-2018 Lead Peer Writing Consultant; Writing Center, Washington State University
- Created, presented, and lead discussion workshops for undergrad students.
 - Work with Professors to create workshops in tandem with student curriculum.
- 2017 Research Intern, PI: Julie Mcelrath, Fred Hutch Cancer Research Center, Seattle, WA
- Researched and assisted *in vitro* T-cell functional assays for live cell flow cytometry sorting.
 - PCR and Gel electrophoresis (setup and documentation).
 - RNA column purification and cDNA synthesis.
 - Cell counting via Guava cell counter.
 - Sterile tissue culture technique.
- 2015-2016 Undergraduate Research Assistant, PI: John Hinson & Paul Whitney, Washington State University, Pullman
- Assisted in electroencephalography set up to study top-down processing.
 - Assisted in administering tests designed to test stress levels in gambling situations.

Awards and Honors

- 2014 Washington State University Scholarship for Academic Merit
- 2015 Washington State University Scholarship for Academic Merit

Community Engagement

- 2017-2018 VP of Society for the Advancement of Chicano and Native Americans in STEM (SACNAS) student organization, Pullman, WA
- 2012-2014 Evergreen Hospital Volunteer, Kirkland, WA